Internal strain monitoring of filament wound pressure tanks using embedded fiber Bragg grating sensors

Dong-hoon Kang
Korea Railroad Research Institute, Uiwang-si, Gyeonggi-do, Republic of Korea

Cheol-ung Kim
Hyundai-Kia Motors, Hwaseong-si, Gyeonggi-do, Republic of Korea

Sang-wuk Park & Chun-gon Kim
Korea Advanced Institute of Science and Technology, Daejeon, Republic of Korea

ABSTRACT: In-situ structural health monitoring of filament wound pressure tanks were conducted during water-pressurizing test using embedded fiber Bragg grating (FBG) sensors. We need to monitor inner strains during working in order to verify the health condition of pressure tanks more accurately because finite element analyses on filament wound pressure tanks usually show large differences between inner and outer strains. Fiber optic sensors, especially FBG sensors can be easily embedded into the composite structures contrary to conventional electric strain gages (ESGs). In addition, many FBG sensors can be multiplexed in single optical fiber using wavelength division multiplexing (WDM) techniques. We fabricated a standard testing and evaluation bottle (STEB) with embedded FBG sensors and performed a water-pressurizing test. In order to increase the survivability of embedded FBG sensors, we suggested a revised fabrication process for embedding FBG sensors into a filament wound pressure tank, which includes a new protecting technique of sensor heads, the grating parts. From the experimental results, it was demonstrated that FBG sensors can be successfully adapted to filament wound pressure tanks for their structural health monitoring by embedding.

1 INTRODUCTION

Recently, the use of filament wound pressure tanks is increasingly prevalent because of high specific strength and specific stiffness over their metal counterparts, as well as excellent corrosion and fatigue resistance. The main applications of filament wound pressure tanks are fuel tanks, a kind of composite structure, has the complexity in damage mechanisms and failure modes. Most of the conventional damage assessment and nondestructive inspection methods are time-consuming and are often difficult to implement on hard-to-reach parts of the structure. For these reasons, a built-in assessment system must be developed to monitor the structural integrity of critical components constantly.

Fiber optic sensors (FOSs) have shown a potential to serve as real time health monitoring of the structures. They can be easily embedded or attached to the structures and are not affected by the electromagnetic field. Also, they have not only the flexibility in the selection of the sensor size but also high sensitiveness. Recently, fiber optic sensors have been introduced to composite structures (Kang et al. 2000, Park et al. 2000). Among many fiber optic sensors, FBG sensors based on wavelength-division-multiplexing technology are attracting considerable research interest and appear to be ideally suitable for structural health monitoring of smart composite structures. FBG sensors are easily multiplexed and have many advantages such as linear response, absolute measurement, etc. Among many researches on filament wound pressure tanks, only a few were performed using FBG sensors.

The temperature and strains were measured during the cure and ingress/egress methods for a standard testing and evaluation bottle were investigated using FBG sensors. Through a water-pressurizing test, experimental data were compared with the results of ESGs and finite element analysis results (Foedinger et al. 1999). The unbalanced strain was calculated from the wavelength difference of a pair of FBG sensors during a water-pressurizing test (Lo et al. 2000). However, it was impossible to measure absolute strains at each sensor position. An FBG sensor was embedded between the hoop layers and used for measuring the internal pressure of the tank through a water-pressurizing test form the wavelength shift of an FBG sensor (Degrieck et al. 2001). The lack of sensors limited strain measurements onto local positions. In addition, they conducted a 3-point bending test of carbon/epoxy composite laminate. Using attached 32 FBG sensors on the filament wound pressure tank as 4 channels, the strains of a filament wound pressure tank were measured through a water-pressurizing test (Kang et al. 2002). From the above literatures, it can be found out that only a few FBG sensors were used when embedding

sensors into the pressure tank and relatively a large number of FBG sensors were used when attaching sensors on the surface. Moreover, problems on FBG sensor signals, especially peak split induced by birefringence and strain gradients occurred in a dome part during a water-pressurizing test. Therefore, it is necessary to monitor the strains of a filament wound pressure tank using a number of embedded FBG sensors in real time without peak split problems.

In this paper, the strains of a filament wound pressure tank were monitored using a number of embedded FBG sensors in real time during the water-pressurizing test and the strain results measured by FBG sensors were compared with those by ESGs and FEM analyses.

2 FABRICATION OF FILAMENT WOUND PRESSURE TANKS

2.1 *Fabrication of FBG sensor lines*

Among several fabrications of FBG sensors, fabrication using a phase mask, devised by (Hill et al. 1993), is currently the most prevalently employed approach because it is suitable for mass production and is simple to handle. However, the grating parts of an FBG sensor can be easily broken by transverse stress applied on the optical fiber. Due to the reason, FBG sensors embedded into a filament wound pressure tank are easy to fail because of the applied tension in reinforcing fibers. In this paper, a revised fabrication process of FBG sensors that is focused on the improvement of sensor survivability during the embedment of FBG sensors is introduced. For this purpose, several processes concerning the fabrication and the embedment are revised.

First, an optical fiber used for fabricating an FBG was substituted to a photosensitive optical fiber (PS1250/1500, Fibercore) because the hydrogen loading process of optical fibers affected on the mechanical strength of them. Second, a sensor line with multiple sensors was fabricated not by the splicing between FBG sensors, but by a simultaneous fabrication of FBG sensors in a single fiber. Generally, optical fibers connected by arc-fusion splicing showed strength degradation to the transverse stress. Third, as a reinforcement of FBG sensors during the embedment, the protection with an adhesive film was conducted as a 2nd protection process after recoating with acrylate. Lastly, optical fibers were extracted from a filament wound pressure tank towards both directions of a sensor line. It was because optical fiber lines were the weakest at the ingress/egress point after the end of curing process.

Figure.1 An FBG sensor line fabricated with a revised process.

Figure 1 shows an FBG sensor line fabricated by a revised fabrication process mentioned in the above paragraph.

2.2 *Filament wound pressure tank with embedded FBG sensor lines*

A filament wound pressure tank consists of a forward dome, an aft dome, a cylinder, and a skirt for joining with other structures. In this paper, a tank is fabricated by the wet winding process using a 4-axis filament winding machine controlled by a computer. The winding tension was 1.5kg/end and the bandwidth of hoop and helical layer was 10.0, 10.5(*mm*) for 5-ends, respectively. The cylinder part includes a 3-body helical layers and 7-body hoop layers so that the sequence is $[(\pm 27.5)_3]_T$ for helical layers and $[90_2/(\pm 45)_2/90_3]_T$ for hoop layers denoting from inner to outer layers. Figure 2 shows the embedded sensor lines during the fabrication process.

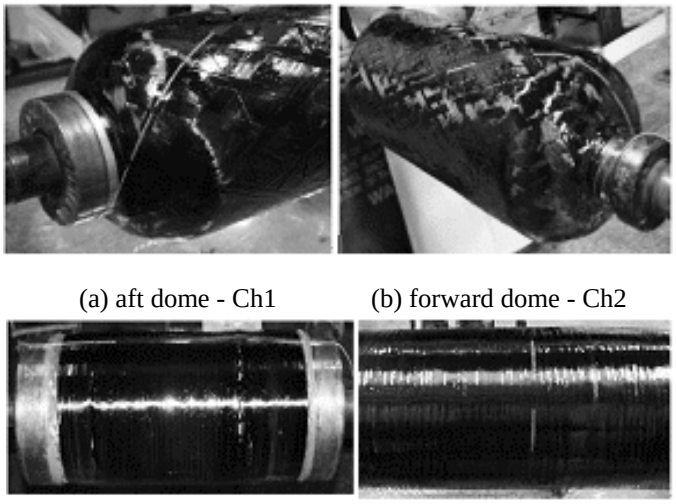

(a) aft dome - Ch1 (b) forward dome - Ch2

(c) cylinder : axis dir. - Ch3 (d) cylinder : hoop dir. - Ch4

(e) the whole configuration

Figure. 2 Embedded FBG sensor lines during the fabrication.

Seven channels of FBG sensors were embedded into a tank. The channel 1(Ch1) and channel 2(Ch2), each has 3 FBG sensors, were embedded between the layer 1 and 2 at aft dome and the layer 2 and 3 at forward dome, respectively. The channel 3(Ch3), which has 3 FBG sensors, was embedded into axis direction of a cylinder part and 3 more lines were used as spare channels (Ch5, 6, 7) because FBG sensors are the weakest when they are embedded perpendicular to the reinforcing fiber like the case of a Ch3. The channel 4(Ch4), which has 4 FBG sensors, was embedded into hoop direction of a cylinder part.

After embedding each sensor line, embedded positions of FBG sensors were measured accurately using a laser pointer. The filament wound pressure tank with embedded FBG sensor lines were cured under rotating condition in the curing cycle ; 80°C(1hr)→120°C(1hr)→150°C(3hrs) in an oven.

Figure 3 shows the configurations of a tank including sensor positions. From the Fig. 3, 'F' denotes FBG sensor and 'E' denotes ESG. And, the figure following 'F' means the channel number.

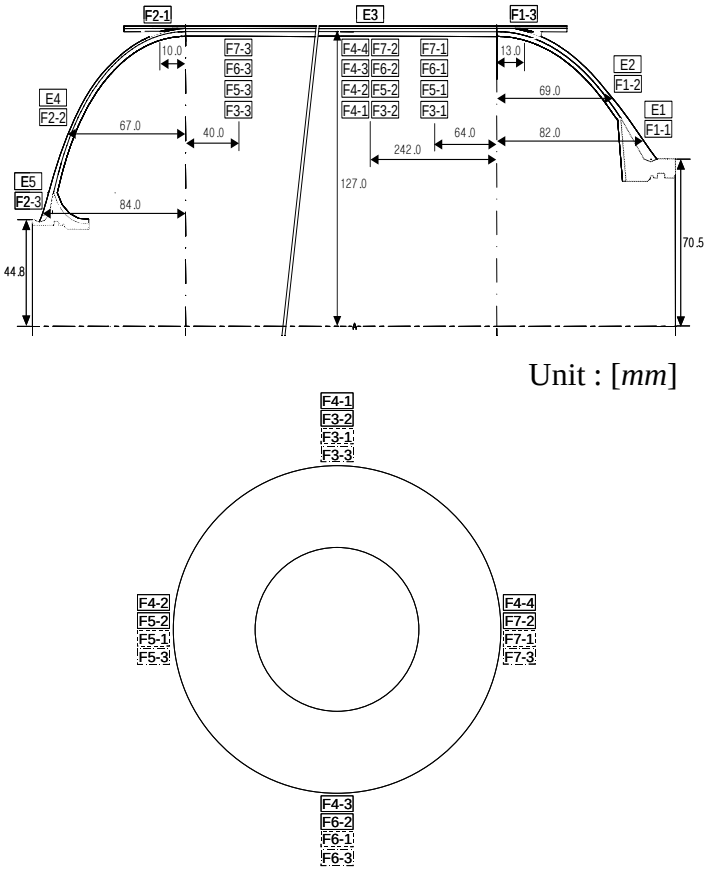

Figure. 3 Configurations and sensor positions.

When embedding FBG sensors into a filament wound pressure tank, especially a dome part, the signal stability of FBG sensors is very important for the strain measurement because there exists a strain gradient in a dome part due to its geometric shape during the water-pressurizing. However, the effects of strain gradient decrease as the grating length of an FBG sensor decreases (Kang et al. 2005). In addition, FBG sensors with shorter grating lengths are more effective when they are embedded perpendicular to the reinforcing fibers. For the reason, two kinds of grating lengths were used such as 10*mm* and 5*mm*. All sensors except those of a Ch4 were fabricated as FBG sensors of 5*mm* gage length.

When the STEB was completely fabricated, 22 of 22 (100%) sensors survived through the whole fabrication processes such as embedding, curing, and mandrel separation. From the wavelength shift of FBG sensors between before and after curing process, residual strains were measured at all sensor positions. As shown in Table 1, compressive strains were measured except the channels of axis direction in cylinder part and the strain values were about hundreds of micro strains. The residual strains in forward dome were relatively higher than those in aft dome. It is noticeable that FBG sensors embedded perpendicular to the reinforcing fiber can be affected not by compressive strains but by tensile strains during the cure, as shown in the results of Ch5 and Ch6.

Table 1. Residual strains of a fabricated tank.

Ch	Sensor No.	Residual strain ( )	Ch	Sensor No.	Residual strain ( )
Ch1	F1-1	-229.1	Ch5	F5-1	52.5
	F1-2	-47.1		F5-2	-82.6
	F1-3	-185.5		F5-3	-622.5
Ch2	F2-1	-457.1	Ch6	F6-1	-351.1
	F2-2	-451.3		F6-2	-550.0
	F2-3	-326.3		F6-3	361.5
Ch3	F3-1	-200.3	Ch7	F7-1	-423.7
	F3-2	-395.2		F7-2	-175.2
	F3-3	-262.3		F7-3	-481.1
Ch4	F4-1	-109.2			
	F4-2	-398.2			
	F4-3	-409.5			
	F4-4	-423.6			

3 WATER-PRESSURIZING TEST

After fabricating a pressure tank, a water pressurizing test of STEB was performed to verify the tank itself. Figure 4 depicts the experimental setup for the strain monitoring of a filament wound pressure tank during hydrostatic pressurization. The tank was pressurized at intervals of 100 *psi* up to 1,000 *psi* using a rotary pump. The strain data from the FBG sensors, ESGs, and a pressure transducer were acquired and processed by a computer in real time.

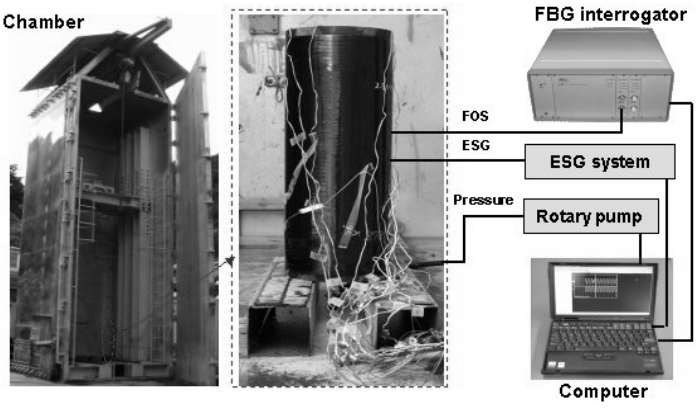

Figure. 4 Experimental setup of water-pressurizing test.

As shown in Fig. 3, 4 ESGs were attached on the dome surfaces at the same locations of embedded FBG sensors, aligned to the helical winding direction. On the cylinder, only 1 ESG was attached in the hoop winding direction, i.e., the circumferential direction of cylinder. The signals of the FBG sensors, strain gauges, and a pressure transducer were acquired simultaneously by computers, processed

and displayed by a signal-processing program written in LabVIEW® software. The specifications of used FBG sensor systems are shown in Table 2.

Table 2. Specifications of an FBG interrogator.

IS-7000 FBG interrogator (FiberPro Co.)	
Wavelength range	35 nm (1530~1565nm)
Average output power	3 mW
Resolution	< 2 pm
Measurement speed	200 Hz
# of channels	8
Temperature range	10 ~ 40℃

4 FINITE ELEMENT MODELING

To compare the strain results measured by FBG sensors and ESGs, finite element analyses on STEB were done by a commercial code, ABAQUS. In this research, the 3-D layered solid element was utilized and the boundary condition was considered as cyclic symmetric. Figure 5 shows the detailed FEA model of STEB realized by a commercial code, PATRAN, and the material properties of T700/Epoxy used in the analysis are as follows.

E_1 = 134.6 GPa, E_2 = 7.65 GPa, G_{12} = 3.68 GPa, ν_{12} = 0.3

σ_f = 2,290 MPa, σ_t = 31.8 MPa, S = 75.8 MPa

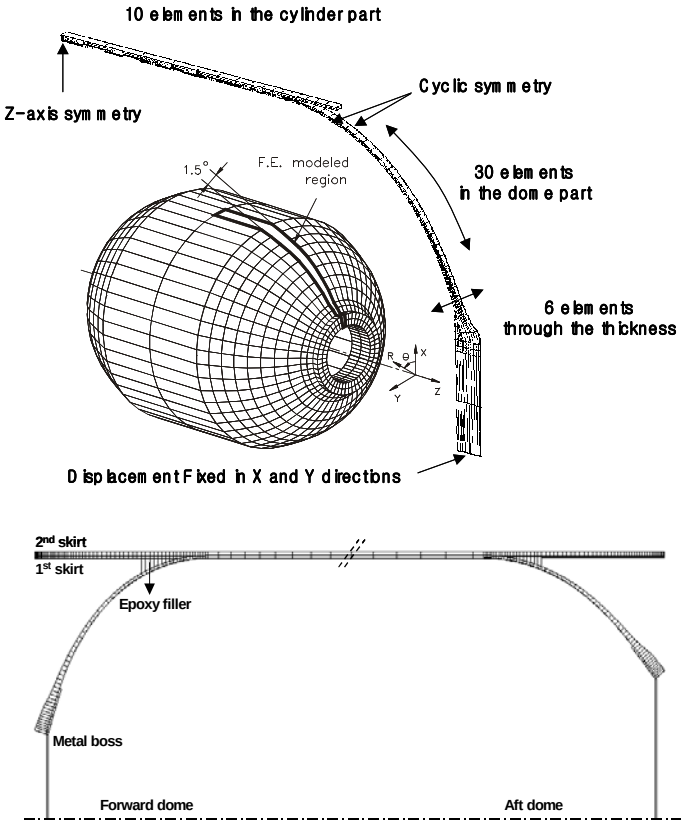

Figure. 5 The FEA model of STEB.

The modified Hashin's failure criterion was selected and applied to progressive failure analysis. For the purpose of failure analysis, a subroutine, USDFLD of ABAQUS ver 6.3 was coded to define the change of mechanical properties due to failure.

5 RESULTS AND DISCUSSIONS

Figure 6 shows strain results measured by FBGs and ESGs in an aft dome. Strains measured by two FBG sensors showed a good agreement with those by ESGs and the strain measured by each FBG sensor showed a good linearity with the increase of pressure.

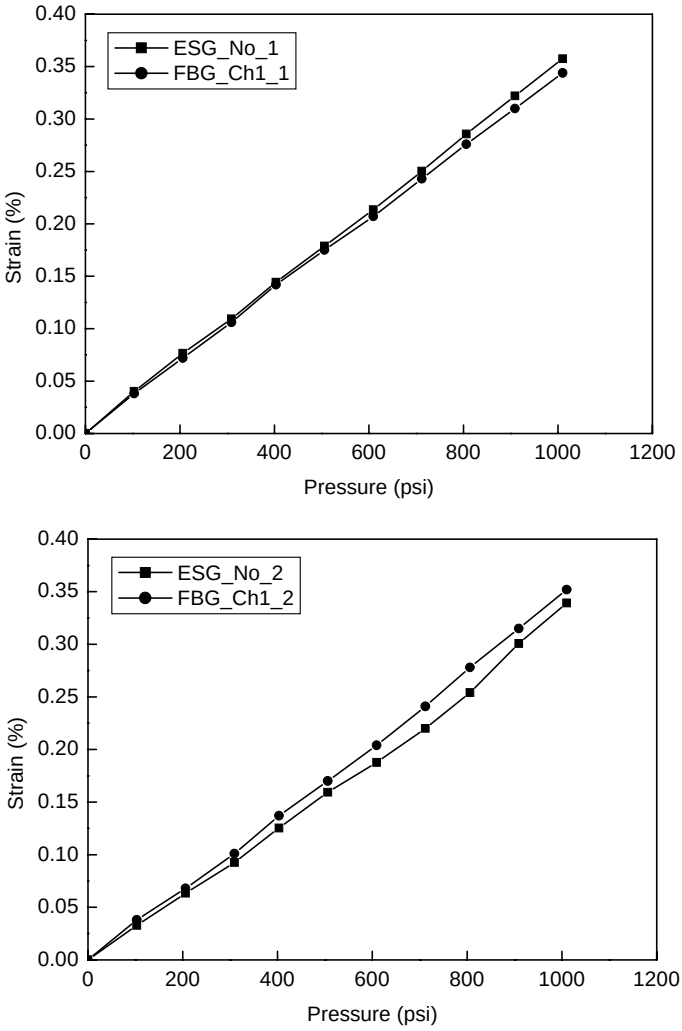

Figure. 6 Strain results of FBG and ESG – aft dome.

In case of a forward dome, as shown in Fig 7, strains measured by two sensors showed a little higher difference than the case of an aft dome. The differences in strains measured by FBG sensors and ESGs may be occurred by a mismatch of attaching angles and locations between them. Also, these differences may be caused by the slippage of an embedded FBG sensor line during the curing process due to resin flow. This can be occurred more easily in a forward dome than in an aft dome because the gradient of a forward dome is steeper.

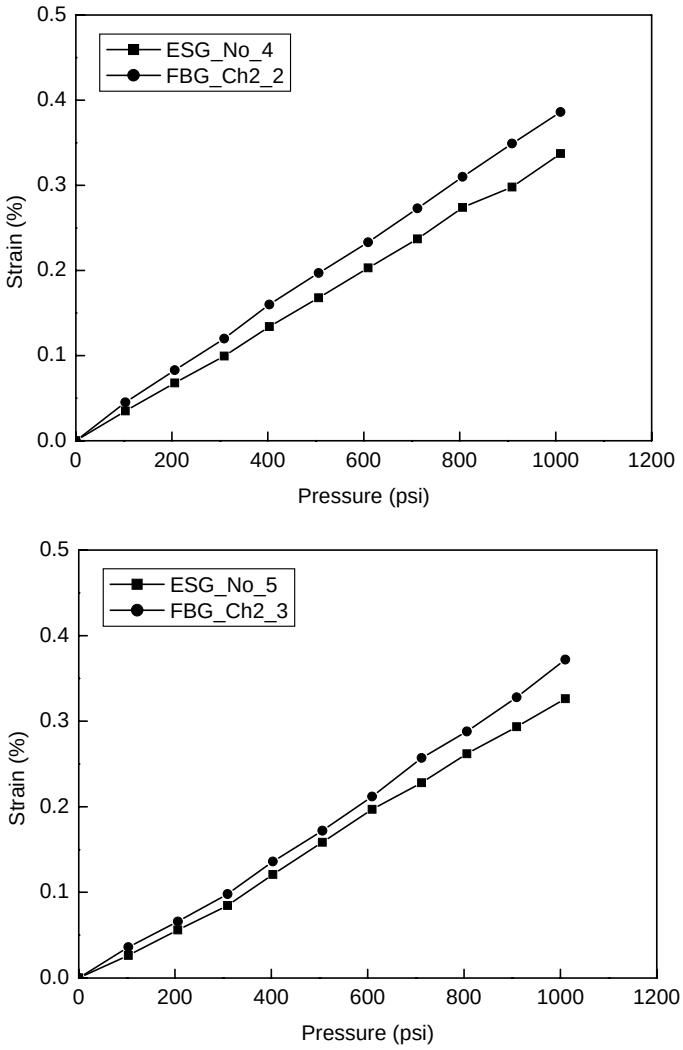

Figure. 7 Strain results of FBG and ESG – forward dome.

Figure 8 shows the strain results of FBGs and an ESG in a cylinder part. Compared with an ESG, two FBG sensors showed a little higher strains and the others lower strains though all sensors showed a good linearity. The reason seems that there occurred a small angle between optical fiber and reinforcing fiber during embedding the Ch4.

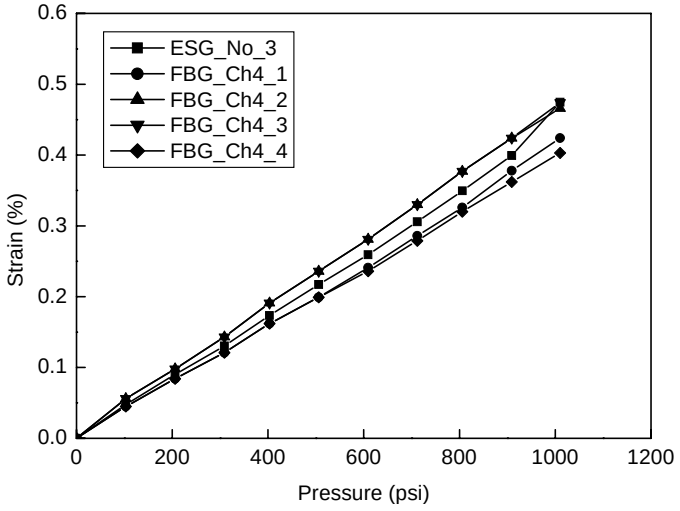

Figure. 8 Strain results of FBG and ESG – cylinder part.

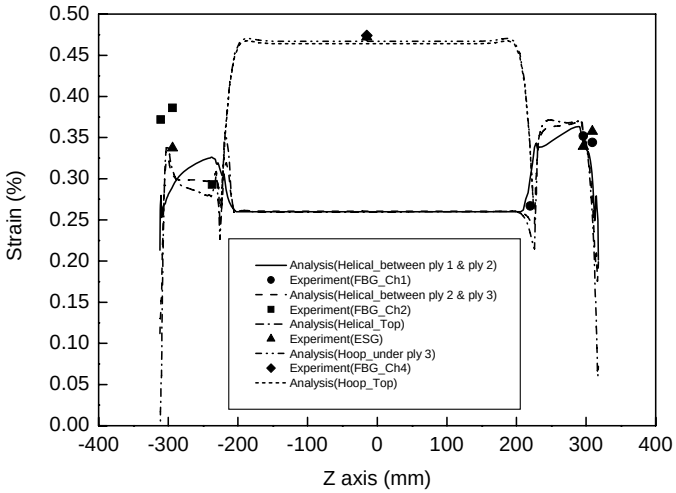

Figure. 9 The results of FBGs, ESGs and FEA at 1,000 psi.

Figure 9 shows the strain results measured FBGs, ESGs, and FEA simultaneously at 1,000 *psi*. The results from FBG sensors were compared with those from ESGs that were attached at the same longitudinal locations with FBG sensors. Both strain results were also compared with those of FEM analyses, which were indicated as lines in Figure 9.

Considering only the FEA results, helical layers of forward dome and aft dome showed a large difference in strains between inner and outer layers. However, there was little difference in strains between inner and outer layers at cylinder part.

In Figure 9, the strains measured by FBGs and ESGs were similar at hoop layers of cylinder part and also showed a good agreement with the FEA results, while the results from FBGs and ESGs at both domes showed a little large difference with each other. As shown in Figure 9, strain changes in both dome parts are very steep in axis direction. Thus, a small error in sensor position can cause large difference in strain results. Nevertheless, the tendency of strain results seems to be agreeable. The errors occurred in this research can be decreased if FBG sensors can be embedded more accurately without any slippage.

Nevertheless, in Figure 9, it is very noticeable that FBG sensors can measure the strain at the positions where the measurement is impossible with ESGs, for example, between the layers of dome and cylinder, the junction part. And, this is very important advantage of FBG sensors, especially in a filament wound pressure tank because it has a severe change in strains between layers of dome part.

6 CONCLUSIONS

FBG sensors totaled 22 in 7 channels were embedded into the domes and cylinder parts of a filament

wound pressure tank in order to measure the strains in real time during hydrostatic pressurization. When embedding multiplexed FBG sensor lines into a filament wound pressure tank, some fabrication steps with sensor line protection were introduced to increase the survivability of FBG sensors.

From the experiment, the strain data from FBGs showed close agreement with the data from ESGs and the results were also verified by the finite element analyses. Through the results, it was successfully demonstrated that the FBG sensors could be useful for the internal strain monitoring of filament wound structures that require a large number of sensor arrays.

ACKNOWLEDGEMENTS

The authors would like to thank the Ministry of Science and Technology, Korea for financial support through a grant from the 21C Frontier R&D Project.

REFERENCES

Kang, H.K. 2000. Development of fibre optic ingress/egress methods for smart composite structures. *Smart Materials and Structures* 9(2): 149-156.

Park, J.W. 2000. Detection of buckling and crack growth in the delaminated composites using fiber optic sensor. *Journal of Composite Materials* 34(19): 1602-1623.

Foedinger, D.L. 1999. Embedded fiber optic sensor arrays for structural health monitoring of filament wound composite pressure vessels. *Proc. Of SPIE* 3670: 289-301.

Lo, Y.L. 2000. Pressure vessel wall thinning detection using multiple pairs of fiber Bragg gratings for unbalanced strain measurements. *Journal of Nondestructive Evaluation* 19(3): 105-113.

Degrieck, J. 2001. Monitoring of fibre reinforced composites with embedded optical fibre Bragg sensors, with application to filament wound pressure vessels. *NDT&E International* 34: 289-296.

Kang, H.K. 2002. Strain monitoring of filament wound composite tank using fiber Bragg grating sensors. *Smart Materials and Structures* 11(6): 848-853.

Hill, K.O. 1993. Bragg gratings fabricated in monomode photosensitive optical fiber by UV exposure through a phase mask. *Applied Physics Letters* 62(10): 1035-1037.

Kang, D.H. 2005. The signal characteristics of reflected spectra of fiber Bragg grating sensors with strain gradients and grating lengths. *NDT&E International* accepted.